THE ASTROPHYSICAL JOURNAL, 472:389–397, 1996 November 20

THE PECULIAR BEHAVIOR OF THE LARGE-SCALE COMPONENTS OF THE SOLAR MAGNETIC FIELD AS A RESULT OF ROSSBY VORTEX EXCITATION BENEATH THE CONVECTION ZONE

E. M. TIKHOMOLOV AND V. I. MORDVINOV
Institute of Solar-Terrestrial Physics, SD RAS, Irkutsk, 664033, P.O. Box 4026, Russia
Received 1995 September 11; accepted 1996 February 28

ABSTRACT

To interpret the dynamical features of large-scale magnetic fields, Rossby vortices are considered. Rossby vortices are assumed to be excited and sustained within a thin layer beneath the convection zone as a result of heating from the solar interior and deformation of the covection zone lower boundary.

Numerical calculations show that a Rossby cyclone generates a large-scale magnetic structure, whose horizontal size compares with the solar radius. The distribution of the vertical component of the magnetic field bears a resemblance in this case to the cloud distribution in the cyclones that are observed in the Earth's atmosphere. A magnetic field with the sign of trailing polarity flux of the local bipolar magnetic regions and a field with the sign of leading polarity are generated, respectively, at the center of the Rossby cyclone and at the periphery. The drift of the cyclone toward the Sun's pole, caused by the Rossby wave emission, leads to a corresponding drift of the large-scale magnetic structure. Longitudinally averaged magnetic field distribution also drifts poleward and has a form of "double surge." The leading polarity is the first to reach the pole. The rotation of the first Fourier components of magnetic field calculated for the low- and midlatitude belts resembles in this case the real picture during the threefold polar field reversal in solar activity cycle.

Rossby cyclones are used also to simulate some other situations on the Sun when, according to observational data, there are weak drifts of the longitudinally averaged component and corotation of the first Fourier components of the low- and midlatitude belts.

Subject headings: MHD — Sun: activity — Sun: interior — Sun: magnetic fields

1. INTRODUCTION

Many solar phenomena substantiate the conclusion that along with the mechanism bringing about the 11 year change of the large-scale component of the magnetic field (LCMF), there are some other processes giving rise to complicated and often unpredicted behavior of the LCMF. One of the manifestations of these processes is the appearance of different rotation of the nonaxisymmetric components of the magnetic fields in different latitude belts (Antonucci, Hoeksema, & Scherrer 1990) and changes of the rotation periods in some special time intervals (Mordvinov & Tikhomolov 1992, 1994). The next is the appearance of poleward drift of a longitudinally averaged radial component of the magnetic field distribution (i.e., axisymmetric component [AC]) after the polar field reversal (Howard & LaBonte 1981; Makarov & Sivaraman 1989). These dynamical properties of the LCMF may be conceived as the deviations from the smooth, idealized change of magnetic fields during the 11 year solar cycle; thus, they can be referred to as the peculiar, or anomalous, phenomena. At present, there are some models that could interpret the peculiar behavior of the nonaxisymmetric component (Ruzmaikin, Sokolov, & Starchenko 1988) and AC (Wang, Nash, & Sheeley 1989), but there is no theory yet that could interpret them on the unified physical basis.

A new impetus to the advancement of the theory for generation of solar magnetic fields was given by helioseismology. Its results provided a new picture of the rotation rate in and beneath the convection zone (Libbrecht & Morrow 1991). A knowledge of the real structure of flows within the solar envelope is important for developing both the theory of an 11 year solar cycle and the theory that could interpret the peculiar behavior of the LCMF.

According to the latest data, the transition from differential rotation (that is independent of the depth throughout the convection zone thickness) to solid-body rotation occurs in a rather thin layer at the base of the convection zone. At present, the structure of this transition layer that was referred to by Spiegel & Zahn (1992) as the tachocline is being studied intensively because it is in this region that the magnetic field which has an 11 year period of changing can be generated (DeLuca & Gilman 1991). Much attention is also given to the study of the so-called penetrative convection layer (Zahn 1991) that lies below the convection zone and is also small in thickness. The importance of this layer for the dynamo theory of an 11 year solar cycle stems from the fact that there occurs a sharp decrease of values of the effective coefficients of turbulent viscosity and heat conductivity as compared with those within the thickness of the convection zone. Nevertheless, the coefficients remain much larger than their molecular values (DeLuca & Gilman 1991).

At present, both the thickness of the tachocline and the exact depth at which strong radial gradients of rotation rate originate are unknown. In this connection, it is still unclear to what extent the tachocline and penetrative convection zone overlap. Most likely, the external boundaries of the zones do not coincide. The absence of large radial gradients of angular rotation velocity and the small viscous damping in the layer between the tachocline and the upper boundary of the penetrative convection zone permits, in principle, the existence of different kinds of hydrodynamical flows there. These flows, we believe, are not passive noise disturbances; rather, they play an active role in the generation of large-scale solar magnetic fields. Therefore, the layer under consideration between the tachocline and the upper boundary of the penetrative convection zone will be referred to as the active transition layer (ATL). In particular, the long-lived large-scale Rossby waves or vortices can exist in the ATL, for which an approximate balance of Coriolis force and pressure gradient is realized in the tangential direction. The scale of these vorticies can be comparable with the solar radius.

Rossby vortices in the case of a small viscous damping have an important property, namely, a long (compared with the rotation period of the spherical envelope) lifetime (Pedlosky 1982). This property permits us to treat them as possible sources of some long-lived global magnetic structures and the reason of peculiar behavior of the LCMF. We suppose that the magnetic field that is driven by the dynamo mechanism of an 11 year solar cycle penetrates to the ATL from the lower boundary. The magnetic field is modulated by the Rossby vortices and then is transferred to the photosphere through the convective envelope. Obviously, the magnetic field transport through the convection zone to the photospheric surface can be accompanied by the distortion of magnetic structures formed by Rossby vortices. The differential rotation in latitude in the bulk of the convection zone can lead to stretching of the magnetic field around the sphere. In addition, the identification of the sources of magnetic fields is also made difficult by small-scale short-lived formations that are particular intense at low heliolatitudes. So we can expect that in some cases it is impossible to obtain information about the real spatial structure of sources using the photospheric data without special processing. But we can expect that in these cases the information about long-lived Rossby vortices will be preserved at least in the dynamics of the largest scale components of magnetic field distribution on the solar surface.

In the approach under consideration, one of the fundamental problems is the mechanism for excitation and sustaining of the Rossby vortices in the ATL. In the absence of such a mechanism, the vortical flows are damped out due to viscosity and interaction with upper and lower lying layers. But the presence of a heat flux from the solar interior imparts to the ATL the property of an open dissipative system, in which the formation of dissipative structures is, in principle, possible (Haken 1978).

For Earth's condition, the baroclinic instability mechanism has long been known, which leads to the excitation of large-scale vortical flows (Pedlosky 1982). However, its realization on the Sun requires a rather large temperature difference between the pole and the equator (Gilman 1969) which is not observed on the solar surface (Altrock & Canfield 1972; Appenzeller & Schroter 1967; Falciani, Rigutti, & Roberti 1974). Therefore, this mechanism is most likely inoperative in the ATL. It is likely that the question of the excitation and sustenance of Rossby vortices cannot be solved without due regard for mutual influence of the convection zone and the ATL. In our opinion, an important factor that leads to the realization of a positive feedback between the ATL and the convection zone and to an enhancement of a small, initial vortical large-scale disturbance is the appearance of a deformation of the interface between the ATL and the convection zone. This deformation is associated with a perturbation of isopicnic surfaces that appears when the flow is excited. The existence of flows leads also to the distortion of the temperature gradient profile and, consequently, to a change in the local conditions for the excitation of convection near the lower boundary of the convection zone.

The basis for the need to take into account the deformation of the interface between the ATL and convection zone is provided by results obtained in our previous papers (Tikhomolov 1994a, 1995d). In these papers, for a rotating fluid layer heated from below and having a deformable upper free surface, a new mechanism of excitation and sustenance of large-scale vortical flows in the Rossby regime was found. The boundaries in this case are kept at a constant temperature, which corresponds to the approximation of infinite heat conductivity of the medium making contact with the layer. The realization of this mechanism, the so-called deformational instability (Golovin, Nepomnyashchy, & Pismen 1994; Tikhomolov 1995d) does not require any other restrictions in addition to those that are usually used when describing the evolution of hydrodynamical flows in rotating thin layers (Gilman 1969). Because of the appearance of a new property, Rossby waves or vortices acquire the character of dissipative structures (Tikhomolov 1994b, 1995b). The revealed mechanism likely can be applied also to the ATL if the convection zone can be represented as a medium with very large heat conductivity. With a sufficiently large difference in values of effective coefficients of turbulent heat conductivity in the ATL and the convection zone, this approximation is quite admissible. The deformed upper boundary of the layer that was considered in the papers of Tikhomolov (1994a, 1995d) is associated with the deformed interface between the ATL and the convection zone.

In this paper, we will not analyze relatively complicated processes of appearance and sustenance of vortical flows and their interaction with convective motions considered in the previous papers (Tikhomolov 1994a, 1994b, 1995b, 1995d) or processes of penetration of the magnetic field through the lower boundary of the layer and its transport upward from the upper boundary. We will consider the dynamics of already-formed Rossby vortices and the distortion by them of some initial magnetic field distribution. The effect of excitation of vortices in this paper for the sake of simplicity will be "turned off."

In our previous papers, we demonstrated the possibility that global magnetic structures can be generated by Rossby vortices (Tikhomolov 1995a) and the possibility of interpreting, using them, solar phenomena of poleward drift of the longitudinally averaged component of the magnetic field (Tikhomolov 1995c). In this paper, we will continue to simulate the generation of magnetic fields by Rossby vortices under different conditions. But the main purpose will be the comparison of the dynamics of the largest scale characteristics of solar magnetic field distributions with the same characteristics calculated for model distributions. As has been noted above, the comparison of behavior of these characteristics very often is the only way to obtain information about the physical origins of sources of the LCMF.

2. GENERATION OF GLOBAL MAGNETIC STRUCTURE BY A ROSSBY CYCLONE

To describe flows in the ATL, we consider a Cartesian model of a rotating fluid layer. The layer is considered to be isolated from external effects. The lower and upper boundaries are presumed to be, respectively, deformed and undeformed free surfaces. To describe the evolution of flows within the layer, we employ the equation in a beta plane approximation for deformation of the upper free surface (Williams 1985). With regard to the scale of global magnetic structures, the following units of measurement are used: for the horizontal coordinates x and y, the size of the order of one-third the solar radius $R \approx 2 \times 10^{10}$ cm; for the vertical coordinate z, the thickness of the layer of Rossby vortex excitation h_0; and for time, $t_0 = 1$ yr ≈ 13 solar rotations. In these units, the dimensionless equation for deformation of the upper surface of the layer has the form:

$$\frac{1}{Q} h_t - \Delta h_t - YJ(h, \Delta h) - B(1 + h)h_x + D_v \Delta^2 h = 0 ,$$

$$\Delta = \partial^2/\partial x^2 + \partial^2/\partial y^2 , \quad J(f, g) = f_x g_y - f_y g_x , \quad (1)$$

where $Q = (r_R/R)^2$ is the Froude number, $r_R = (gh_0)^{1/2}/2\Omega$ is the Rossby-Obukhov deformation radius, g is gravity, Ω is the angular rotation velocity, $Y = 2\Omega t_0 Q$, B is the parameter characterising the beta effect, the dependence of angular velocity on latitude, $D_v = \nu t_0/R^2$, and ν is the coefficient of effective turbulent kinematic viscosity. For the chosen units of measure and solar parameters, we have $Q \approx 1$ and $Y \approx 150$. The parameter B is taken as $B = 35$. The coefficient ν in the layer that is the part of the penetrative convection zone is specified an order of magnitude smaller than that usually taken within the convection zone thickness (Gilman & Miller 1986). In this case, $D_v \approx 0.1$. Hence, the typical time of the viscous damping of large-scale vortices is comparable with the duration of a solar cycle.

For the sake of definiteness, it is assumed that the beta plane resides in the northern hemisphere, so that the direction from the lower edge of the figures to the upper edge along the y-axis corresponds to the direction from the helio-equator to the north pole. The results are represented in the frame of reference moving with the velocity corresponding to 30° of latitude. Coordinates in latitude and longitude are given in degrees.

The differential rotation profile is specified as follows:

$$h_{\rm shr} = -H_{\rm shr}[(y^3 - y_{30}^3)/3 - (y_{30} + y_{90})(y^2 - y_{30}^2)/2 + y_{30} y_{90}(y - y_{30})] , \quad (2)$$

with the zero velocity value on the upper boundary and a change in the velocity direction at 30°. Such a velocity distribution simulates qualitatively the linear rotation velocity profile determined from observations (Gilman & Miller 1986). The parameter of the differential rotation profile is taken to be $H_{\rm shr} = 3$. On the upper and lower boundaries, conditions for the absence of differential rotation perturbations are specified. The equations are solved numerically by a spectral method on a grid of 361×90 points. The grid step in this case corresponds to 1°. A periodic boundary condition is assumed in the coordinate x which is an analog of the longitude.

With the differential rotation profile existing on the Sun, a longer lifetime corresponds to cyclonic rather than anticyclonic large-scale vortical formations (Tikhomolov 1995a). Therefore, in this paper we study the evolution of cyclones. In the first series of calculations, at the initial instant of time we specify, at the background of a sheared flow, a cyclone of a Gaussian shape at the latitude 20° which has the size $2d = 15°$ and the amplitude $H_0 = -0.5$.

Figure 1 shows the evolution of the cyclone with the time. The cyclone is transported by differential rotation and, as a result of the Rossby wave emission, it is drifting in the poleward direction (Pedlosky 1982).

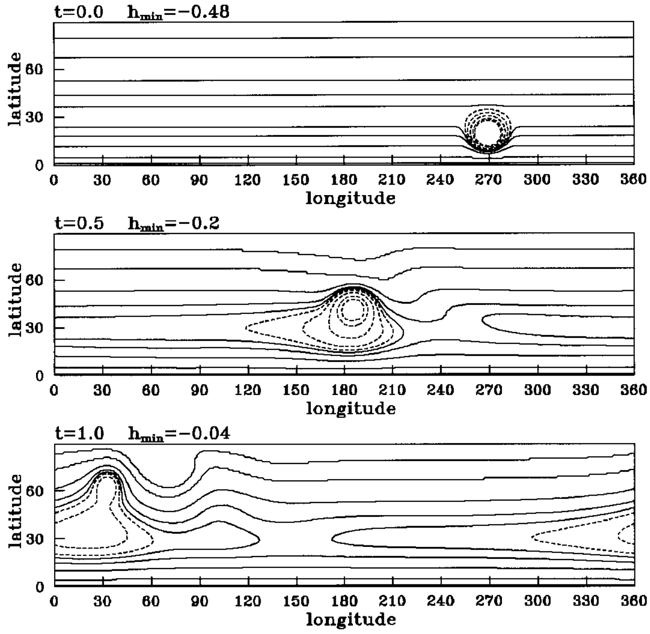

FIG. 1.—Evolution of a Gaussian cyclone, specified at the initial instant of time at the latitude 20° and having the amplitude $H_0 = -0.5$ and the size $2d = 15°$. Shown are the isolines of disturbances of the upper surface of the layer: ± 0.005, ± 0.02, ± 0.05, ± 0.1, and ± 0.14. Solid and dashed lines show, respectively, positive and negative values of the quantities. Time and minimum values of the quantities are indicated above the top edges of the figures.

Rossby vortices are capable of generating a magnetic field because of the presence of ageostrophic components of the flow (Tikhomolov 1995a). For ease of the calculations, the horizontal components of the magnetic field are represented as the sums $B^x = -T_y + P_x$, $B^y = T_x + P_y$ (Gilman 1969). The component of the function T, independent of x, gives an axisymmetric field which corresponds to a toroidal field assumed in many dynamo models (Priest 1982). The component of the function P, independent of x, gives an axisymmetric field in meridional planes, which corresponds to a poloidal field. Therefore, in what follows we will call T and P, respectively, the toroidal and poloidal functions. The value of the vertical component of the magnetic field on the upper surface of the layer is inferred by the formula $B^z = -\Delta P$. The unit of measurement of the horizontal components of the magnetic field B^x and B^y is represented by the characteristic value of the magnetic field strength M, while the unit of measurement of the vertical component B^z is represented by the quantity δM, where $\delta = h_0/R$.

The equations for magnetic field generation by hydrodynamical flows in a thin layer for the toroidal T and the poloidal P functions have the form (Tikhomolov 1995a)

$$\Delta T_t = -\Delta(uT_x + vT_y) - \Delta(uP_y - vP_x) - (v\Delta P)_x + (u\Delta P)_y + D_m \Delta^2 T , \quad (3)$$

$$\Delta P_t = -u\Delta P_x - v\Delta P_y + w_x T_y - w_y T_x + D_m \Delta^2 P , \quad (4)$$

where $D_m = \mu t_0/R^2$, and $\mu \approx \nu$ is the effective coefficient of turbulent magnetic diffusion. In this paper, we neglect the back influence of the magnetic field upon hydrodynamical flows using the approach employed in kinematic dynamo theory (Priest 1982). Velocity components in the coordi-

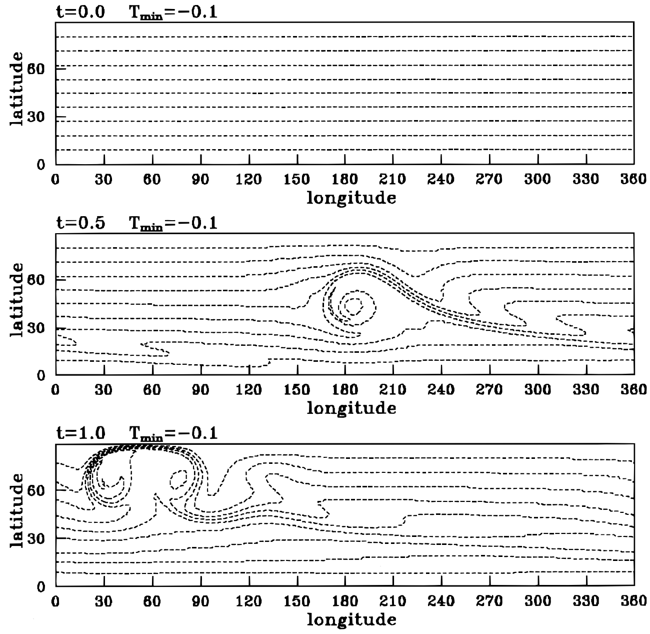

FIG. 2.—Evolution of the toroidal function for the flows shown in Fig. 1. Shown are the isolines: 0, −0.01, −0.02, −0.03, −0.04, −0.05, −0.06, −0.07, −0.08, and −0.09. Time and minimum values of the quantities are indicated above the top edges of the figures. The initial conditions are described in the text.

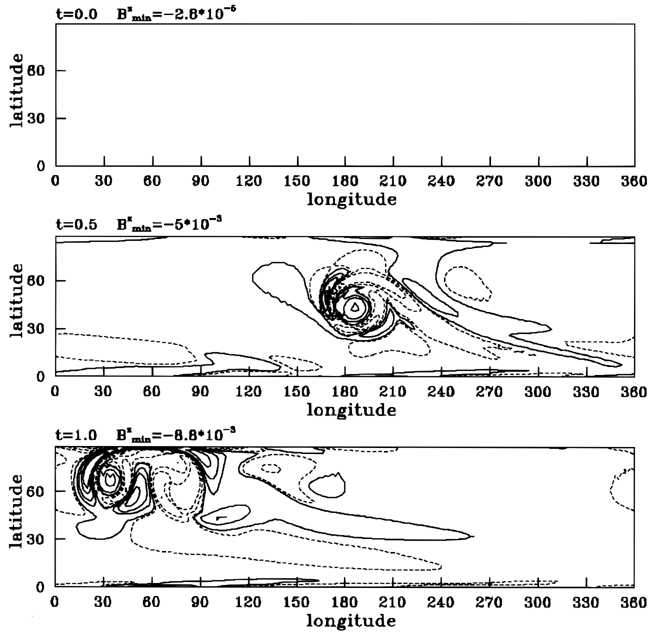

FIG. 4.—Evolution of the vertical component of the magnetic field generated by the flows shown in Fig. 1. Solid and dashed lines show, respectively, positive and negative values of the quantities. Shown are the isolines: $\pm 10^{-3}$, $\pm 2 \times 10^{-3}$, $\pm 4 \times 10^{-3}$, and $\pm 6 \times 10^{-3}$. Time and minimum values of the quantities are indicated above the top edges of the figures. The initial conditions are described in the text.

nates x, y, z that are substituted into equations for the magnetic field are determined in the present case, respectively, by the formulas $u = -Yh_y$, $v = Yh_x$, $w = h_t$. At the initial instant of time, the toroidal and poloidal functions are specified as being independent of the coordinate x:

$$T_{\rm dyn} = T^0_{\rm dyn} \frac{y}{y_{90}} , \tag{5}$$

$$P_{\rm dyn} = P^0_{\rm dyn} \left(\frac{y}{y_{30}} - 1 \right)^3 . \tag{6}$$

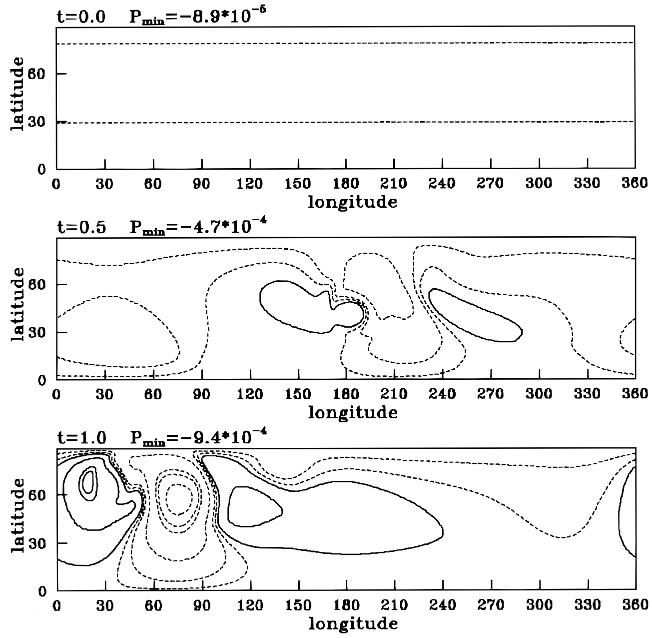

FIG. 3.—Evolution of the poloidal function for the flows shown in Fig. 1. Solid and dashed lines show, respectively, positive and negative values of the quantities. Shown are the isolines: 0, $\pm 5 \times 10^{-5}$, $\pm 2 \times 10^{-4}$, $\pm 5 \times 10^{-4}$, $\pm 6 \times 10^{-4}$, and $\pm 8 \times 10^{-4}$. Time and minimum values of the quantities are indicated above the top edges of the figures. The initial conditions are described in the text.

The polarity distribution of the vertical component of the magnetic field at the initial instant of time corresponds to the polarity distribution of the AC following the polarity field reversal in an 11 year cycle of solar activity (Howard & LaBonte 1981). Magnetic field lines in this case connects regions below and above the latitude 30°.

The parameters $T^0_{\rm dyn}$ and $P^0_{\rm dyn}$, by virtue of the linearity of the equation for the magnetic field, can be chosen relatively arbitrarily. The restriction imposed by dynamo theory and observations is a large ratio of the amplitude of the toroidal to poloidal component of the magnetic field. In this paper, it was assumed that $T^0_{\rm dyn} = -0.1$, $P^0_{\rm dyn} = -10^{-5}$. With the chosen initial destribution of the toroidal and poloidal functions, the negative sign corresponds to the leading polarity of emerging local bipolar magnetic regions, and the positive sign corresponds to the trailing polarity. Such a distribution of the signs was observed in cycles 20 and 21, respectively, in the northern and southern hemispheres, in periods of time following the polarity field reversal.

Boundary conditions on the upper and lower edge for the toroidal and poloidal functions are specified in much the same way as the boundary condition for deformation of the upper free surface of the layer: on the boundaries there are no perturbations of the values specified at the initial instant of time.

The evolution of the toroidal and poloidal functions, calculated in accordance with equations (3) and (4), in the presence of flows shown in Figure 1, is presented, respectively, in Figures 2 and 3. In the first stage, isolines of the toroidal function are curled into a spiral, which corresponds to spiraling of the horizontal component of the magnetic field, in much the same manner as observed in numerical calculations of Miura (1984) and Wu (1986). Subsequently, because of the presence of magnetic diffusion, magnetic field lines reconnect to form closed configurations. For the poloidal function, the formation of closed isolines is also observed.

Figure 4 shows isolines of the vertical component of the magnetic field B^z. Spiraling is well defined. The picture resembles very much the outline of cyclones observed in Earth's atmosphere, only with the magnetic field rather than clouds being a tracer in the case being considered. A field with the sign of trailing polarity is produced at the center of the vortex, and a field with the sign of leading polarity is generated at its periphery. As will be shown later in the text, such a structure leads to a certain alternation of the sign of the AC.

3. THE DYNAMICS OF THE FIRST FOURIER COMPONENTS OF THE LOW- AND MIDLATITUDE BELTS AND OF THE AXISYMMETRIC COMPONENT IN SOLAR ACTIVITY CYCLES 20–22 AND ITS SIMULATION

Next we will compare model calculations with observations. As was pointed out in the Introduction, in some cases a direct comparison of experimental data with calculations seems to be impossible, and it is necessary to invoke methods of large-scale filtering of the distribution of solar magnetic fields. A limiting case of such filtering that preserves important properties of the sources of the LCMF is the calculation of the first Fourier component (FFC) in different latitude belts with maximum spatial period in longitude (or dipole components of the latitude belts) and AC. To calculate the FFC of the latitude belt with the size in latitude 30°, we follow the method used in the paper by Mordvinov & Tikhomolov (1992).

The change in phase of the FFC characterizes the rotation of the sources of the LCMF, while the evolution of the AC is representative of the displacement of sources in the latitudinal direction. The change of FFC phase has a relatively simple form, if one large-scale magnetic region predominates in the belt. Otherwise, it is necessary to use higher order harmonics.

The generation of global magnetic structures in model calculations also gives rise (after having been expanded in terms of harmonics) to the FFC and AC. It is reasonable to suggest that by comparing the dynamics of these largest scale components with similar characteristics obtained from experimental data, it will become possible to speak of the reality of the proposed interpretation of sources of the LCMF.

Plots of time variation of rotation of the FFCs of latitude belts with size in latitude 30° for solar cycles 20, 21, and 22 are presented in Figures 5*a*, 5*c*, 6*a*, and 6*c*. We used magnetograpic (Hoeksema & Scherrer 1986) and processed Hα data (Mordvinov & Tikhomolov 1992). The plus signs denote the phase of the FFCs calculated for midlatitude belts 30°–60° for each Carrington rotation. Open circles denote the phase of the FFCs calculated for the low-latitude belts 0°–30° (for the southern hemisphere in the 21st cycle, the belt 10°–40°). When selecting low-latitude belts, we take into consideration the results reported by Antonucci et al. (1990), who found a different character of rotation of magnetic fields in low-latitude belts of the northern and southern hemispheres in solar activity cycle 21. For the sake of convenience, when determining the rotation period from the slope of the trajectories, the plots are repeated three times in the direction of the *y*-axis. Trajectories pertaining to the same hemisphere are plotted on the same figure.

Isolines of the AC that are determined from digitized synoptic maps by simple longitudinal averaging are shown in Figures 5*b* and 6*b*. Solid lines show isolines corresponding to the positive sign of the field, and dashed lines correspond to the negative sign. The axis of ordinates indicates the sine latitude. Figures 5*d* and 6*d* show the Wolf number dynamics and number of the cycles.

Let us note the main dynamical features of the FFC and AC which are well defined in Figures 5 and 6.

1. During the solar cycles, there are long time intervals in which the FFCs of the latitude belts of size 30° have a stable rotation period. During some time intervals, the FFCs of the neighboring belts corotate with the rotation period larger than or of the order of the Carrington period.
2. Changes in rotation occur relatively often during short time intervals of about a few solar rotations. Such events are denoted in Figures 5 and 6 by vertical bars.
3. Changes in rotation occur most often simultaneously in neighboring latitude belts.
4. During some time intervals, the drift of the AC leads to a change of sign of the polar field (Howard & LaBonte 1981; Makarov & Sivaraman 1989). Simultaneously, typical variations in rotation of the FFCs of neighboring latitude belts occur.

The character of the plots in Figures 5 and 6 and the dependence of the instants of variations of rotation periods on the relative values of the phases of the FFCs indicates that the FFCs in each of the belts seem to be formed by real physical sources that are of a reasonably large size. This hypothesis is supported also by the correlation between the appearance of drifts of the AC and variations in rotation periods of the FFCs of neighboring latitude belts.

Next we will compare the dynamics of the FFCs and the ACs obtained from experimental data with those calculated in a model described in § 2. In doing so, for the vertical component of the magnetic field being calculated we will apply the same technique for obtaining FFCs and the ACs as used when treating experimental data.

3.1. *Simulation of the Rotation of the FFCs of the Mid- and Low-Latitude Belts During the Threefold Polar Field Reversal*

The distribution of the vertical component of the magnetic field, generated by a single cyclone, has a relatively complicated vortical structure (Fig. 4). If this distribution were unchanged with time, then one would expect a sufficiently simple behavior of the FFC and AC. However, a strong nonstationarity of the flow and a variation in the cyclone's shape and amplitude can lead to significant fluctuations of the phase of the FFCs of the neighboring belts. An additional factor that adds complexity to the picture is the distortion of the magnetic field distribution far from the cyclone center by secondary flows which are formed as a result of the Rossby wave emission. Therefore, in principle, even a single vortex is able to form a rather complicated

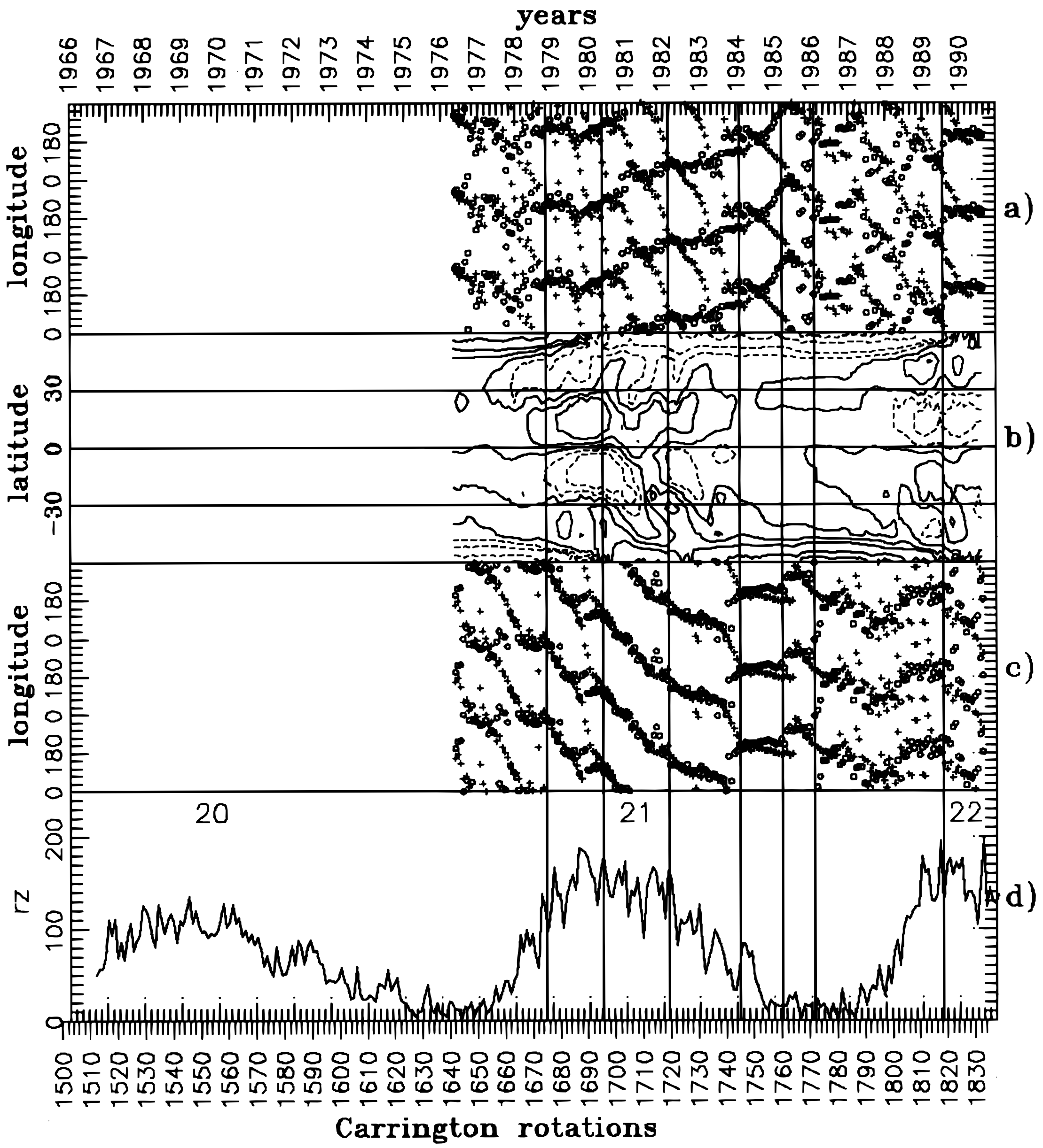

FIG. 5.—Dynamics of the large-scale component of the magnetic field in solar activity cycles 21–22 as determined from magnetic data. The designations are described in the text.

pattern of behavior of FFCs of neighboring latitude belts. Therefore, in this paper we will confine ourselves to modeling the dynamical features of the LCMF using only one cyclone specified at the initial instant of time.

In this subsection, we will report results derived by a treatment of the calculation presented in Figures 1–4. Figures 7*a*–7*b* show the rotation of the FFCs of two neighboring belts, 0°–30° and 30°–60°, and isolines of the longitudinally averaged value of the vertical component of the magnetic field determined for configuration shown in Figure 4. The results are represented in a frame of reference rotating with the velocity corresponding to the latitude 15°. The rotation period at this latitude for the Sun is close to the Carrington period. When calculating the AC, presented in Figure 7*b*, to eliminate short-period fluctuations, we carried out a sliding averaging on the time interval corresponding to one Carrington rotation and on a spatial scale corresponding to 5°. The axis of ordinates in Figure 7*b*, as in Figures 5*b* and 6*b*, indicates the sine latitude. Instants of typical variations of the dynamics of the FFC and AC are shown by vertical bars.

The time variation of the AC shows a typical "double surge" similar to that observed in the northern hemisphere in solar activity cycle 20 (Figure 6). A poleward drift of the leading polarity field was observed during that period after mid-1969, followed by a trailing polarity drift (Howard & LaBonte 1981). From the beginning to the end of 1971, when the drift of both polarities was most pronounced, the FFCs of neighboring latitude belts rotated with a period close the Carrington period. Subsequently, following the termination of the threefold polar field reversal (Makarov & Sivaraman 1989), there occurred a mismatch of the rotation of the FFCs. The FFC of the midlatitude belt began to rotate with a period larger than the Carrington period, while the FFC of the low-latitude belt rotated with a period smaller than the Carrington period.

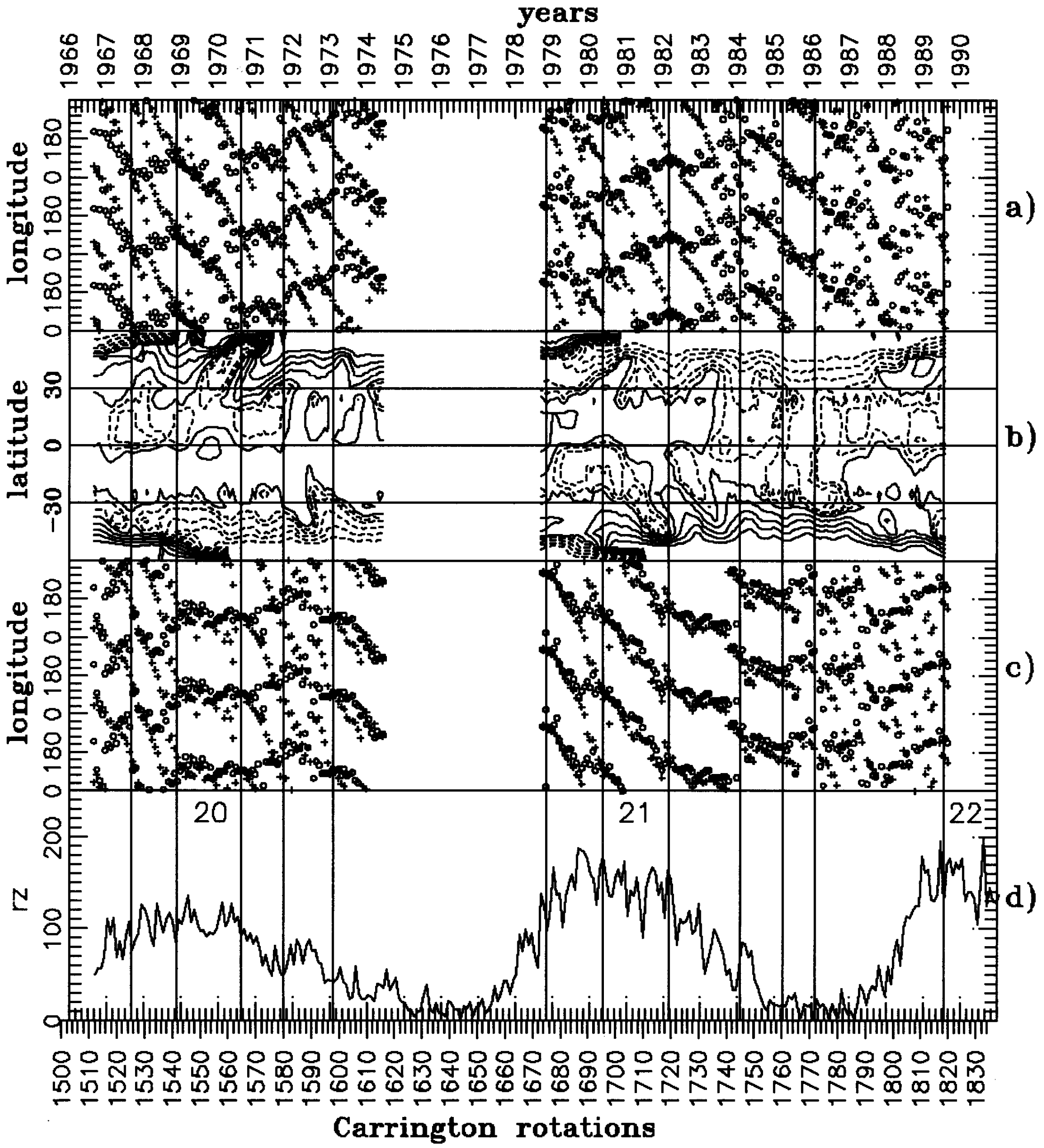

FIG. 6.—Dynamics of the large-scale components of the solar magnetic field in solar activity cycles 20–22 as determined from Hα data. The designations are the same as in Fig. 5.

In model calculations, to the period of the drift of both polarities and the correlated behavior of the FFC, there corresponds the time interval from $t = 0.17$ to $t = 0.68$ labeled by vertical bars. As has been shown above, such a picture of the transfer of the AC is determined by the structure of the field generated by the cyclone (Fig. 4). Before time $t = 0.17$ in model calculations, there occurs the establishment of a vortical picture of the distribution of the vertical component of the magnetic field. The jump in the phase of the FFC of the low-latitude belt at time $t = 0.68$ is associated with diminution of the influence of the cyclone upon the low-latitude belt as a consequence of its poleward drift. From this time on, secondary flows that generate a magnetic field in the low-latitude belt acquire a great influence upon the phase of the FFC of the low-latitude belt. A gradual deceleration of rotation of the FFC of the low-latitude belt, well visible after time $t = 0.68$, is also associated with the drift of the cyclone.

3.2. *Modeling of the Corotation of the FFCs of the Mid- and Low-Latitude Belts with a Period Larger than the Carrington Period During the Weak Drift of the AC*

As experimental data show, a variation in the rotation period of the FFCs of the neighboring latitude belts is not always accompanied by a pronounced drift of the ACs. In particular, such a situation occurred after mid-1972, when both the FFCs of low-latitude belts decelerated their rotation, and the drift of the AC with the sign of leading polarity was not perceptible (Fig. 6). Another example is the poleward drift of the field with the sign of leading polarity in the southern hemisphere of the Sun between mid-1980 and the beginning of 1982 which, likely, did not lead to the polar field reversal (Figs. 5 and 6).

For a numerical simulation of such situations, it suffices to decrease the amplitude of the initial disturbance. At the initial instant of time, we specify a cyclone by the amplitude

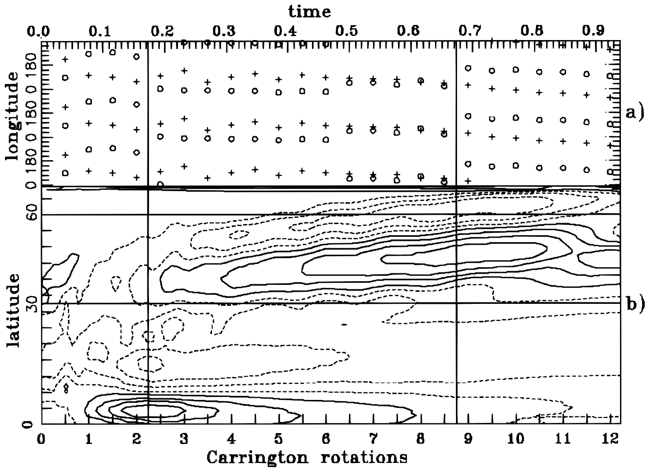

FIG. 7.—(*a*) Rotation of the first Fourier components of the magnetic field of the low- and midlatitude belts for the distribution of the vertical component of the magnetic field shown in Fig. 4. The designations are the same as in Fig. 5*a*. (*b*) Evolution of the longitudinally averaged value of the vertical component of the magnetic field. The designations are the same as in Fig. 5*b*. Shown are the isolines: 0, $\pm 5 \times 10^{-5}$, $\pm 10^{-4}$, $\pm 1.5 \times 10^{-4}$, and $\pm 2 \times 10^{-4}$.

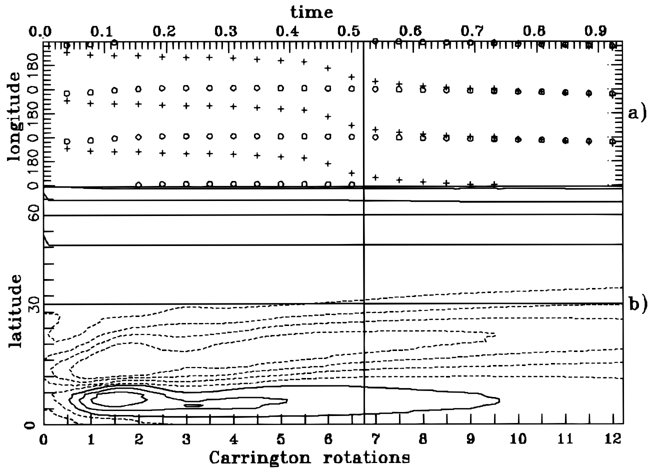

FIG. 9.—(*a*) Rotation of the first Fourier components of the low- and midlatitude belts when a weak cyclone at the latitude 15° is specified at the initial instant of time. The designations are the same as in Fig. 5*a*. (*b*) Evolution of the longitudinally averaged value of the vertical component of the magnetic field. The designations are the same as in Fig. 5*b*. Shown are the isolines: 0, $\pm 2 \times 10^{-5}$, $\pm 4 \times 10^{-5}$, and $\pm 6 \times 10^{-5}$.

$H_0 = 0.05$ at the latitude 30°, of the size of 15°. The calculated dynamics of the FFC and AC is shown in Figures 8*a*–8*b*. The period of establishment is followed (from $t = 0.13$ on) by a corotation of the FFCs of the low- and midlatitude belts with a rotation period larger than the Carrington period, which is caused by the influence of the cyclone upon both latitude belts.

The cyclone distorts the initial distribution of the AC; however, the drift of the AC is much less pronounced than in a previous calculation (note that isolines in Fig. 8*b* depict a field that is an order of magnitude smaller than that in Fig. 7*b*). After time $t = 0.63$, as in a previous calculation, there is a desynchronization of the rotation of the FFCs of the neighboring latitude belts. This attributed also to a decrease of the cyclone's amplitude and to a corresponding reduction in its influence upon the low-latitude belt.

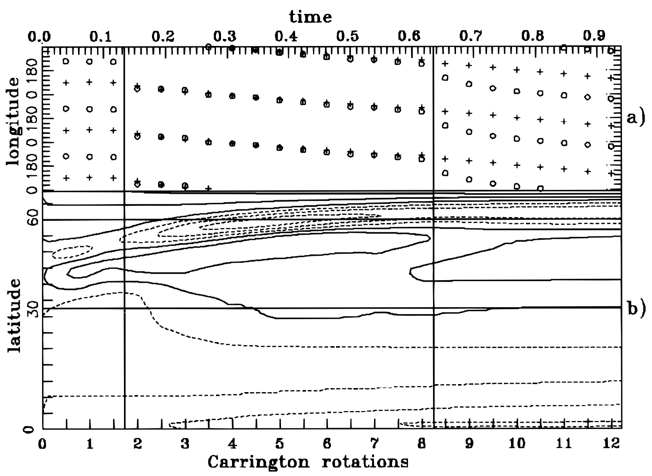

FIG. 8.—(*a*) Rotation of the first Fourier components of the low- and midlatitude belts when a weak cyclone at the latitude 30° is specified at the initial instant of time. The designations are the same as in Fig. 5*a*. (*b*) Evolution of the longitudinally averaged value of the vertical component of the magnetic field. The designations are the same as in Fig. 5*b*. Shown are the isolines: 0, $\pm 2 \times 10^{-5}$, $\pm 4 \times 10^{-5}$, and $\pm 6 \times 10^{-5}$.

3.3. *Modeling of the Corotation of the FFCs of the Mid- and Low-Latitude Belts with a Period of the Order of the Carrington Period in the Absence of a Drift of the AC*

In the model calculations considered above, one can trace clearly the role of the cyclone's amplitude in the realization of one or another picture of the dynamics of the FFC and AC. It would be interesting also to follow the variation of the picture of the dynamics of the large-scale components of the magnetic field by specifying the vortex at the initial instant of time at low latitudes. In this case, it should be expected that, as a result of its influence upon the midlatitude belt, a corotation of both belts with a period of the order of the Carrington period will be observed.

For modeling this situation, at the initial instant of time we specified the cyclone at latitude 15°, of the size $2d = 10°$, and with the amplitude $H_0 = 0.05$.

The dynamics of the FFCs of neighboring latitude belts and of the AC for this variant of calculations is shown in Figures 9*a*–9*b*. In a certain time after the beginning of the calculations, there occurs a perturbation of the flow in the midlatitude belt and the formation of the rotation of FFC of this belt with a period larger than the Carrington period. However, as the perturbation in the midlatitude belt decays, there occurs a synchronization of the rotation of the FFCs of the neighboring belts, and at time $t = 0.52$ they begin to corotate with a period of the order of the Carrington period. As in a previous calculation, because of the smallness of the amplitude of the initial cyclone, its poleward drift is weak, and there is no pronounced drift of the AC.

This variant of calculations simulates the dynamical picture of the large-scale components that occurred in the southern hemisphere in cycle 20 from the beginning of 1969 to mid-1970, and in cycle 21 from the beginning of 1982 to the end of 1983. In those periods, the FFCs of the neighboring belts rotated with the Carrington period (Figs. 5 and 6).

4. CONCLUSIONS

The calculations carried out both in this paper and in previous publications (Tikhomolov 1995a, 1995c) show that simulations of the dynamics of the large-scale components of the magnetic field based on Rossby vortices have considerable opportunity for interpreting some real situations on the Sun.

It would be very appealing to compare the magnetic structures, generated by Rossby vortices, with the structures seen directly on the photosphere. The results published, for example, by Mogilevsky et al. (1986) point out the possibility of comparison of large-scale vortical structures seen on the solar surface with those obtained in model calculations. But more often a direct comparison of model configurations of magnetic field and synoptic maps does not seem to be possible because of the distortion of generated magnetic structures when the field is transferred through the convection zone (that hinders also direct observations of hydrodynamical vortices) and because of the presence of a small-scale component in the distribution of magnetic fields on the photospheric surface.

However, as calculations show, Rossby cyclones, as least, can be used to simulate different variants of the behavior of the largest scale components of the distribution of solar magnetic fields. The appearance of distinct rotation periods of the first Fourier components of different latitude belts or the disappearance of these periods are due, respectively, to excitation or decay of Rossby vortices. Rossby vortices are assumed to be excited and sustained within a thin layer beneath the convection zone as a result of heating from the solar interior and deformation of the convection zone lower boundary. Depending on the amplitude of cyclones and their position in latitude, a different behavior of the first Fourier component of low- and midlatitude belts and the axisymmetric component is possible.

With a sufficiently large amplitude, the cyclone (and the associated magnetic structure) is drifting poleward. In this case, the time evolution of the axisymmetric compondent appears as a "double surge" of fields with opposite signs (Wang et al. 1989). The leading polarity field is the first to reach the pole. The dynamics of the AC and FFC resembles in this case the real picture of the large-scale field dynamics during the threefold polar field reversal in solar activity cycle 20 (Howard & LaBonte 1981; Makarov & Sivaraman 1989).

With a weaker amplitude of the cyclone, the effects of corotation of the FFCs of the neighboring belts with a period of the FFC of the midlatitude or low-latitude belt are possible according to the latitude of the excitation of the vortex. In this case, the poleward drift of the AC can be weak or even absent.

The results obtained suggest the reality of the interpretation of peculiar behavior of the LCMF of the Sun as a consequence of the excitation of Rossby vortices in the thin layer beneath the convection zone.

It seems likely that Rossby vortices can be used also to interpret the facts of a correlated behavior of large-scale magnetic fields in the low-latitude belts of different hemispheres. The basis for this is provided by calculations of the dynamics of Rossby waves in Earth's atmosphere, showing the possibility of their propagation across the equator (Grose & Hoskins 1979). For solar conditions in the presence of a magnetic field this phenomenon will produce the effect of a close correlation of the behavior of magnetic fields in different hemispheres. Such an effect was observed in cycle 21, but it manifested itself especially clearly in solar cycle 20, when during more than 4 years the low-latitude belts of the northern and southern hemispheres had the same large-scale structure (Mordvinov & Tikhomolov 1990).

This work has been done under support of the Russian Foundation for Fundamental Research, grant number 93-92-17014.

REFERENCES

Altrock, R. C., & Canfield, R. C. 1972, Sol. Phys., 23, 257

Antonucci, E., Hoeksema, J. T., & Scherrer, P. H. 1990, ApJ, 360, 296

Appenzeller, I., & Schroter, E. H. 1967, ApJ, 147, 1100

DeLuca, E. E., & Gilman, P. A. 1991, in Solar Interior and Atmosphere, ed. A. N. Cox, W. C. Livingston, & M. S. Matthews (Tucson: Univ. Arizona Press), 275

Falciani, R., Rigutti, M., & Roberti, G. 1974, Sol. Phys., 35, 277

Gilman, P. A. 1969, Sol. Phys., 8, 316

Gilman, P. A., & Miller, J. 1986, ApJS, 61, 585

Golovin, A. A., Nepomnyashchy, A. A., & Pismen, L. M. 1994, Phys. Fluids. 6, 34

Grose, W. L., & Hoskins, B. J. 1979, J. Atmos. Sci., 36, 223

Haken, H. 1978, Synergetics (Berlin: Springer-Verlag)

Hoeksema, J. T., & Scherrer, P. H. 1986, The Solar Magnetic Field–1976 Through 1985/World Data Center A for STP (Boulder, CO: Rep. UAG-94)

Howard, R., & LaBonte, B. J. 1981, Sol. Phys., 74, 131

Libbrecht, K. G., & Morrow, C. A. 1991, in Solar Interior and Atmosphere, ed. A. N. Cox, W. C. Livingston, & M. S. Matthews (Tucson: Univ. Arizona Press), 479

Makarov, V. I., & Sivaraman, K. R. 1989, Sol. Phys., 119, 35

Miura, A. 1984, J. Geophys. Res., 89, 801

Mogilevsky, E. I., Ioshpa, B. A., Starkova, L. I., Utrobin, V. G., Korobova, Z. B., Stoyanova, M. N., & Golovko, A. A. 1986, in Contr. Astron. Obs. Skalnate Pleso, Vol. 15, Proc. 12th Region. Consult. on Solar Phys., ed. A. Antalova (Tatranska Lomnica: Astron. Ustav Slovenskej Akad. Vied), 189

Mordvinov, V. I., & Tikhomolov, E. M. 1990, Issledovaniya po geomagnetizmu aeromii i fizike Solntsa, 91, 33

———. 1992, Sol. Phys., 138, 23

———. 1994, in Poster Papers Presented at the Seventh European Meeting on Solar Physics ed. G. Belvedere et al. (Catania: Catania Astrophys. Observ.), 27

Pedlosky, J. 1982, Geophysical Fluid Dynamics (Berlin: Springer-Verlag)

Priest, E. R. 1982, Solar Magnetohydrodynamics (Dordrecht: Reidel)

Ruzmaikin, A. A., Sokolov, D. D., & Starchenko, S. V. 1988, Sol. Phys., 88, 5

Spiegel, E. A., & Zahn, J.-P. 1992, A&A, 265, 106

Tikhomolov, E. M. 1994a, JETP Lett., 59, 163

———. 1994b, in Lecture Notes in Physics, Vol. 432, Proc. Seventh Europ. Meet. on Solar Phys. Advances in Solar Physics, ed. G. Belvedere, M. Rodono, & G. M. Simnett (Berlin: Springer-Verlag), 91

———. 1995a, Sol. Phys., 156, 205

———. 1995b, Europhys. Lett., 29 (7), 543

———. 1995c, A&A, 301, 277

———. 1995d, Phys. Fluids, submitted

Wang, Y.-M., Nash, A. G., & Sheeley, N. R., Jr. 1989, ApJ, 347, 529

Williams, G. P. 1985, J. Atmos. Sci., 42, 1237

Wu, C. C. 1986, J. Geophys. Res., 91, 3042

Zahn, J.-P. 1991, A&A, 252, 179